**Title:**

# TMEM184B promotes pruriceptive neuron specification to allow itch sensitivity

**Authors:**

Erik G. Larsen[1], Tiffany S. Cho[1], Matthew L. McBride[1], Jing Feng[2], Bhagyashree Manivannan[1], Cynthia Madura[3], Nathaniel E. Klein[1], Elizabeth B. Wright[1], Hector D. Garcia-Verdugo[1], Chelsea Jarvis[1], Rajesh Khanna[3], Hongzhen Hu[2], Tally M. Largent-Milnes[3], and Martha R.C. Bhattacharya*[1]

**Affiliations:**

[1] Department of Neuroscience, University of Arizona, 1040 E 4th Street, Tucson AZ 85721, USA

[2] Center for the Study of Itch and Sensory Disorders, Department of Anesthesiology, Washington University School of Medicine, 660 Euclid Avenue, St. Louis MO 63110, USA

[3] Department of Pharmacology, University of Arizona College of Medicine, 1501 N. Campbell Avenue, Tucson AZ 85724, USA

**Correspondence:** marthab1@email.arizona.edu

**Abstract**

Nociceptive and pruriceptive neurons in the dorsal root ganglia (DRG) convey sensations of pain and itch to the spinal cord, respectively. One subtype of mature DRG neurons, marked by Somatostatin (*Sst*) expression, is responsible for sensing mediators of acute itch and atopic dermatitis, including the cytokine IL-31. How itch-sensitive (pruriceptive) neurons are specified is unclear. Here we show that *Tmem184b*, a gene with roles in axon degeneration and nerve terminal maintenance, is required for the expression of a large cohort of itch receptors, including those for IL-31, Leukotriene C4, and Histamine. Mice lacking *Tmem184b* fail to respond to IL-31, but maintain normal responses to pain and mechanical force, indicating a specific behavioral defect in pruriception. Lineage-tracing studies using *Sst*-driven Cre recombinase show a loss of pruriceptive neurons in *Tmem184b*-mutant mice, suggesting a defect in neuron subtype specification. We identify an early failure of proper Wnt-dependent transcriptional signatures and signaling components in Tmem184b mutant mice that can explain the improper DRG neuronal subtype specification. Lentiviral re-expression of Tmem184b in mutant embryonic neurons restores Wnt signatures, whereas re-expression of Tmem184b in adult DRG fails to restore itch responses. Together, these data demonstrate that Tmem184b promotes adult somatosensation through developmental Wnt signaling and specification of pruriceptive neurons. Our data illuminate a new key regulatory step in the processes controlling the establishment of diversity in the somatosensory system.

**Keywords**: Itch, somatosensory, development, dorsal root ganglia, transcriptomics, behavior, Wnt signaling

## Introduction

Neurons of the somatosensory system are responsible for detecting temperature, touch, pain, and itch. Somatosensory neurons also relay the first warning signals when peripheral tissues are damaged. For example, following a skin wound, local inflammatory processes occur near the terminals of somatosensory neurons, causing the release of cytokines and neuroactive peptides that can either directly depolarize neurons or result in their sensitization to other agonists (Dong and Dong, 2018; Solinski et al., 2019; Wilson et al., 2013). A common consequence of increased skin inflammation is the triggering of itch.

Acute and chronic itch are significant morbidities in humans. Itch-causing pathological conditions have a variety of causes, including skin disorders (atopic dermatitis), drug-induced reactions, systemic disorders such as liver disease, and other neurological disorders (Dong and Dong, 2018). The sensation of itch is distinct from pain and is carried by a subset of itch-specific somatosensory neurons called pruriceptive neurons with cell bodies in the dorsal root ganglia (DRG). Skin itch is triggered by release of pro-inflammatory compounds such as cytokines (IL-4, IL-13, and IL-31), thymic stromal lymphopoietin (TSLP), and histamine from mast cells and epithelial cells, which act upon membrane receptors and channels present in epidermal nerve endings (Oetjen et al., 2017; Solinski et al., 2019; Wilson et al., 2013). In addition to chemical itch, mechanical stimuli can evoke similar itch sensations but rely on a distinct spinal circuit (Acton et al., 2019; Bourane et al., 2015; Pagani et al., 2019; Pan et al., 2019).

To convey these sensations, somatosensory neurons display diversity in both protein expression and nerve terminal morphology. Somatosensory neurons have been classically categorized using soma size, electrical properties (including myelination state), and expression of a few markers that include lectins (IB4), neuroactive peptides, and ion channels. Recently, multiple groups have described the diversity of somatosensory neurons from the adult DRG using single-cell RNA sequencing, a powerful approach that has allowed an improved

classification of subtypes of sensory neurons and their abilities to respond to agonists (Li et al., 2016a; Usoskin et al., 2015). These studies classified DRG neurons into six to eight defined groups based solely on expression of unique transduction or signaling molecules. In addition, by genetically labeling and sorting DRG populations prior to RNAseq, the ion channels conferring unique electrical properties have been mapped to eight distinct populations (Zheng et al., 2019). Finally, developmental single cell profiling of these neurons has recently enabled a first look at possible developmental trajectories of sensory neurons (Sharma et al., 2020). A failure of the sensory neuron diversification process could leave organisms unprepared for their changing environment and susceptible to predation.

One population of DRG neurons identified in these single cell RNAseq studies is uniquely identified by expression of the peptides Nppb (natriuretic peptide B, also called brain natriuretic peptide, or BNP) and Somatostatin (Sst), as well as IL-31 receptor type a (Il31ra) (Li et al., 2016a; Usoskin et al., 2015). These cells, called NP3 or C2 neurons and representing 6-8% of all neurons in the DRG, are purely pruriceptive, transmitting itch, but not pain, signals to the dorsal horn of the spinal cord (Huang et al., 2018; Li et al., 2016a; Usoskin et al., 2015). These neurons develop from an initially *Runx1*$^{+}$, *TrkA*$^{+}$ population that ultimately loses *TrkA* expression but gains peptidergic markers such as Calcitonin gene related peptide (CGRP) (Lallemend and Ernfors, 2012). How this subset is specified remains a mystery.

Transmembrane protein 184b (Tmem184b) is a relatively uncharacterized member of the Transporter-Opsin-GPCR (TOG) superfamily of proteins (Yee et al., 2013). Tmem184b is required for efficient axon degeneration following nerve injury, and also for proper sensory and motor nerve terminal maintenance (Bhattacharya et al., 2016). In mice lacking *Tmem184b*, nociceptive terminals in the epidermis show swollen endings, and mice show deficits in broad measures of sensorimotor behavior (Bhattacharya et al., 2016). Here we show that Tmem184b controls the expression of a large cohort of sensory receptors in the DRG, specifically those in the NP3/C2 population mediating pruriception. We found specific behavioral defects in acute

itch, but not pain, when *Tmem184b* is absent, showing that Tmem184b is required for proper pruriception. Tmem184b loss causes a reduction in the total number of NP3/C2 neurons in adults. We show that Tmem184b is required in embryonic neurons for expression of critical drivers of sensory neurogenesis, suggesting an early role for Tmem184b in sensory development. Rescue experiments in both adults and embryos support a primary role for Tmem184b in pruriceptive neuron specification through control of Wnt signaling. Our data identify a critical role for Tmem184b in the establishment of the neurons responsible for primary pruriception.

## Results

### Tmem184b is Required for Expression of Pruriceptor-Specific Markers

In studying the nervous system phenotypes of loss of the transmembrane protein Tmem184b, which include axon protection as well as dysmorphic nerve terminals (Bhattacharya et al., 2016), we sought to identify expression changes that could contribute to these phenotypes. We performed RNA sequencing on isolated adult DRGs of 6-month-old *Tmem184b* global knockout mice and compared sequences to age-matched wild-type mice. We observed 316 genes with significantly downregulated (FDR ≤ 0.05) transcript expression in *Tmem184b*-mutant ganglia, and 90 genes that had significantly upregulated transcripts (Fig. 1A). Strikingly, the downregulated genes contained a large fraction of markers previously identified in single-cell RNAseq studies as being unique to a population of pruriceptive neurons (called NP3 or C2 in previous studies) (Chiu et al., 2014; Li et al., 2016b; Usoskin et al., 2015). The key markers of NP3/C2 neurons are dramatically downregulated, with reductions in Il31ra, Nppb, and Sst being among the largest changes seen in the dataset (Fig. 1B). However, other types of neurons also showed decreased expression of their unique markers, including NP2/C4 (identified by Mrgpra3) and NP1/C5-6 (identified by Mrgprd) (Fig. 1C). Taken together, this data identifies Tmem184b as a major regulator of somatosensory gene expression, particularly in pruriceptive populations.

To predict the functional significance of these expression changes, we performed pathway analysis using Panther. Downregulated transcripts were enriched in pathways such as GPCR signaling, serotonin receptor signaling, and synaptic transmission (Fig. 1D). When human phenotype ontology was examined, pruritus was the top and most significantly changed feature ($p < 0.003$). These data show that Tmem184b is required for appropriate transcription of signaling pathways critical to normal sensory function.

**Tmem184b is required for itch, but not pain, responses**

To test the behavioral consequences of the expression changes observed in *Tmem184b*-mutant mice, we challenged them with agonists that promote itch or pain. The cytokine IL-31, implicated in atopic dermatitis, activates the IL31RA/OSMR heterodimeric receptor on NP3/C2 DRG neurons, whereas the anti-malarial agent chloroquine (CQ) activates MRGPRA3 on NP2/C4 DRG neurons (Cevikbas et al., 2014; Dillon et al., 2004; Liu et al., 2009). *Tmem184b*-mutant mice are resistant to scratching evoked by IL-31 injection (Fig. 2A). In addition, mutant mice have a reduced response to chloroquine, although the reduction does not reach statistical significance (Fig. 2B, $p = 0.07$). To examine the effects on other nociceptive populations, we performed mechanical threshold and thermal pain testing. *Tmem184b*-mutant mice responded normally to these stimuli (Fig. 2C-E). Taken together, this data shows that Tmem184b is selectively required for behavioral responses to pruriceptive agonists.

**Aberrant cellular responses to nociceptive and pruriceptive agonists in *Tmem184b*-mutant mice**

To determine whether functional shifts in adult somatosensory neuron populations had occurred, we performed calcium imaging on dissociated adult DRG neurons. We saw significant reductions in the percentage of neurons that responded to the broad nociceptive receptor agonists, capsaicin (a TRPV1 agonist) and allyl isothiocyanate (AITC, a TRPA1 agonist) (Fig. 2F-G). The percent of neurons responding to two agonists specific for the NP3/C2 population, CYM5442 (an S1PR1 agonist) and LY344862 (an HTR1F agonist), was reduced (Fig. 2I-J).

These results suggest that cell loss contributes to our pruriceptive phenotypes. Paradoxically, mutant mice showed a small increase in the percentage of neurons responding to both IL-31 and chloroquine (Fig. 2K-L). Because in wild type mice, S1pr1, Htr1f, and Il31ra are all unique markers of NP3/C2 neurons, we interpret these dynamic changes as evidence that receptor gene expression has been at least partially uncoupled with cell fate in *Tmem184b*-mutant ganglia. To rectify the slight increase in the percentage of IL-31 responsive neurons with the loss of behavioral responses, we evaluated the amplitude of IL-31-induced calcium increases in individual neurons. Among neurons classified as responders, IL-31 triggered substantially weaker responses in mutant neurons when compared to wild type (Fig. 2M). The reduction in response magnitude of individual neurons to IL-31 likely contributes to the loss of IL-31-induced pruriception in adults.

**Tmem184b regulates key developmental pathways in somatosensory neurons**

To evaluate whether the somatosensory neurons corresponding to the NP3/C2 population had truly been reduced, we sought to use a genetic fate-mapping strategy to label this population as soon as it arises. NP3/C2 DRG neurons are uniquely marked by Somatostatin expression, therefore we used *Sst*$^{Cre}$ combined with Cre-dependent tdTomato to identify this group of neurons. We found that the percent of adult neurons labeled with tdTomato is reduced but not completely eliminated in *Tmem184b*-mutant mice (Fig. 3A-B). This result supports our calcium imaging data and indicates that reduction of this subpopulation of neurons contributes to the reduction of gene expression seen in RNAseq experiments. When taken together with the calcium imaging data, it suggests that reductions in both neuron numbers and response amplitude contribute to the loss of IL-31 induced pruriception.

We sought to identify the mechanism by which Tmem184b promotes NP3/C2 neuron specification by evaluating gene expression changes during the formation and differentiation of sensory ganglia. In mice, unique DRG subpopulations arise from a uniform group of neural crest precursors over a period of about three weeks in late embryonic and early postnatal life (from

E10-P10) (Lallemend and Ernfors, 2012). Tmem184b is expressed in DRG neurons as early as E11.5 according to a recent single-cell RNAseq study (Sharma et al., 2020); we independently confirmed its expression at E13 in somatosensory ganglia (Fig. 3C). Embryos homozygous for the T184b$^{GT}$ allele show greater than 75% loss of Tmem184b transcripts in DRG at this timepoint. To identify the developmental pathways dependent on Tmem184b, we isolated RNA from embryonic day 13 (E13) dorsal root ganglia and compared transcriptional signatures between mutant and wild type ganglia using RNAseq. We identified 1635 genes for which transcripts significantly changed in the absence of Tmem184b at this timepoint (Adjusted $P < 0.01$) (Fig. 3D). Using pathway analysis, we identified multiple key developmental processes, including axonogenesis and neuronal development and differentiation, that are substantially affected by the loss of Tmem184b at E13 (Fig. 3E-F). These results underscore that Tmem184b controls key aspects of the establishment of the somatosensory system.

One of the main pathways controlling neurogenesis and differentiation of DRG is Wnt signaling. Neuronal precursors undergo two waves of neurogenesis stimulated by Wnt pathway activation (Garcia-Morales et al., 2009; Lee et al., 2004); the later wave produces the majority of nociceptors and pruriceptors. Wnt signaling promotes the expression of transcription factors critical in establishing neuronal numbers and identity in migrating neural crest progenitors, including Neurog1 (Ngn1) and Neurog2 (Ngn2) (Kondo et al., 2011; Lallemend and Ernfors, 2012; Lee et al., 2004; Raisa Eng et al., 2001). In *Tmem184b* mutant ganglia, we observe striking reductions at E13 in transcripts for Wnt3a, Ngn1, and Ngn2 (Fig. 3G-I), suggesting that an initial failure in Wnt production could produce deficiencies in the transcriptional programs necessary for nociceptor and pruriceptor development. Tmem184b is required for the proper transcript expression of components at all levels of the Wnt pathway, including ligands (Wnt3a, Wnt4), receptors (Fzd2, Fzd10), and transcription factors (Tlx3, Neurod1) (Fig. 3F and Supp Fig. 1).

To analyze the trajectories of somatosensory neuron populations as they are adopting their adult fates, we combined our E13 analysis with a parallel transcriptomic evaluation of gene expression in developing ganglia at postnatal day 0 and postnatal day 10. At the latest time point, expression of NP3/C2 DRG markers has been previously observed (Lallemend and Ernfors, 2012). Somatostatin expression in wild-type began at P0 and was maintained at high levels through P10, when NP3/C2 neurons express the majority of their unique markers (Fig. 3J). In *Tmem184b*-mutant mice, Sst failed to turn on at P0 but had a burst of expression at P10. This burst of *Sst* expression in mutants at P10 likely causes tdTomato expression, as these neurons would be permanently marked following the burst even though they express little *Sst* as adults (*Sst* transcript levels are 27% of wild-type in adult DRGs, Fig. 1A). In comparison, Il31ra expression is suppressed throughout these developmental timepoints in *Tmem184b* mutants (Fig. 3K). This data argues for a significant loss of NP3/C2 neurons in *Tmem184b*-mutant mice.

Many other genes necessary for somatosensory development or mature function are also dysregulated (Supp Fig. 1). Taken together, our data supports a model in which Tmem184b, acting early in neuronal development, controls a Wnt-dependent developmental program leading to the proper specification of pruriceptive neurons.

**Tmem184b controls expression of Wnt signaling components in embryonic DRG neurons**

To more directly test if Tmem184b activity in DRG neurons controls critical developmental gene expression networks, we performed embryonic rescue of Tmem184b in vitro. We cultured E13 embryonic DRG neurons from wild type or mutant mice for 14 days (DIV 14, roughly equivalent timewise to postnatal day 8) (Fig. 4A). In a subset of neurons from each mutant embryo, we re-expressed Tmem184b using lentiviral transduction on the day of dissociation. At day 14, we collected RNA and performed RNA sequencing for each condition. We identified differentially expressed genes in DIV 14 mutant neurons relative to wild type (Fig. 4B), and in mutant neurons with and without restoration of Tmem184b (Fig. 4C). Within these genes, we identified those that both decreased in the absence of Tmem184b (blue, Fig. 4B) and

were increased in mutants upon re-expression of Tmem184b (gold, Fig. 4C). Our analysis resulted in the identification of 304 genes matching this pattern. Gene ontology analysis revealed biological processes significantly over-represented by these genes, representing processes positively regulated by Tmem184b activity (Fig. 4D). The most over-represented process among genes positively regulated by Tmem184b is the planar cell polarity (PCP) pathway (23.5-fold enriched), a non-canonical Wnt signaling pathway. Canonical Wnt signaling was also enriched in this group of genes (7.93-fold). Tmem184b regulated expression of components at multiple levels of the Wnt pathway, including receptors (Fzd1, Fzd10) as well as transcription factors (Tcf7l2, Taz) (Fig. 4E). Many more genes that positively influence Wnt signaling (green) were identified as compared to those that inhibit Wnt signaling (red). Of note, because these cultures were significantly enriched in neurons over glia (due to the presence of the anti-mitotic factor FdU for the duration of culture), it suggests that the expression changes to Wnt components are likely occurring within the DRG neurons themselves. Many of the processes controlled by Tmem184b also influence critical neuronal functions including calcium regulation (7.86-fold enrichment) and axon guidance (4.18-fold enrichment). This data implicates Tmem184b in controlling key developmental steps in the establishment of the somatosensory system. Our data support a model in which Tmem184b controls the proper expression of Wnt signaling components necessary for the cascade of developmental events leading to pruriceptive neuron differentiation.

### *In vivo* re-expression of Tmem184b in adult mutant ganglia does not increase IL-31 responses

Given our results showing reductions in the NP3/C2 population and effects on Wnt signaling, we sought to evaluate whether Tmem184b contributes primarily to early neuronal specification or if it can influence pruriceptive function in adulthood. If Tmem184b's role is primarily developmental, then re-expression in adults should not be able to rescue IL-31 responsiveness. We constructed an adeno-associated (AAV9) virus encoding *Tmem184b* under

the control of the neuronal-specific Synapsin promoter, and injected this virus, or control AAV9 expressing only mCherry, into the cervical intrathecal space (Fig. 5A). Histological analysis showed that virus was able to spread to DRG from C1-C10 (Fig. 5B) and also into some of the central axonal projections of these DRGs into the dorsal horn (Fig. 5C). Virus expression was also seen in the dorsal gray matter (Fig. 5C). In these mice, we evaluated scratching responses to subsequent IL-31 injection. We noted a slight, though statistically insignificant, rise in IL-31 induced scratching in all AAV-infected mutant mice, indicating that AAV injection and expression may influence the baseline levels of IL-31 responsiveness (Fig. 5D). Surprisingly, we found that in wild-type mice, overexpression of *Tmem184b* attenuates scratching to IL-31 injection. However, we were unable to alter mutant responsiveness with adult re-expression of *Tmem184b*. The failure to rescue in adults is consistent with a primary effect of Tmem184b activity during development of pruriceptive neurons.

**Discussion**

Our data support a significant role for Tmem184b in the control of pruriception. *Tmem184b*-mutant DRGs show reduction of pruriceptor transcripts in the NP3/C2 population. Of note, mRNA expression of the IL-31 receptor subunit, Il31ra, and its co-receptor, Osmr, are both strongly decreased in the absence of *Tmem184b*. We see reduced IL-31-induced scratching as well as lower response magnitudes in individual neurons in response to IL-31 application in mutant mice. IL-31-mediated itch is central to the development of atopic dermatitis, and thus the expression and function of its receptor is of significant medical interest (Dillon et al., 2004). Our data identify a novel mechanism promoting the expression of the IL-31 receptor on sensory neurons and ultimately controlling IL-31 induced behaviors.

Using a genetic labeling strategy, we found that NP3/C2 neuron numbers are reduced in the absence of Tmem184b, though they are not completely eliminated. Using calcium imaging, we found a reduction of nociceptive neurons generally and skewed numbers and/or sensitivity of

remaining pruriceptive populations. In addition, at E13, we see reductions in transcripts encoding critical developmental factors including Wnt3a, Neurog1, and Neurog2. These three factors are essential for the establishment and differentiation of neurons within sensory ganglia (Lallemend and Ernfors, 2012). Based on this evidence, we believe that Tmem184b acts early in sensory development to promote the proper specification of nociceptive and pruriceptive neurons.

Data from embryonic neurons indicate that Tmem184b promotes the expression of Wnt signaling components. Wnt signaling is critical for early neural crest development, and in stem cells, Wnt signaling induces Neurog1, Neurog2, and Pou4f1 (Brn3a) expression (Garcia-Morales et al., 2009; Kondo et al., 2011; Lee et al., 2004). One possibility is that Tmem184b activity affects these pathways via the homeodomain transcription factor, Tlx. Supporting this idea, Tlx3 nociceptor-specific knockouts show loss of pruriceptive populations, and pruriceptive markers showing reduced expression in Tlx3 mutant DRGs significantly overlap with Tmem184b-affected genes (Huang et al., 2017; Lopes et al., 2012). Intriguingly, the effect of blockade of Wnt secretion on the morphology of the mouse neuromuscular junction is strikingly similar to that seen in Tmem184b-mutant mice, further implicating a link between Tmem184b and Wnt signaling (Bhattacharya et al., 2016; Shen et al., 2018). Future experiments should test how Tmem184b activity and appropriate Wnt signaling in early sensory development are associated.

It is possible that Tmem184b plays an additional role in adult nociceptor maintenance. In wild type mice, over-expression of Tmem184b causes reduction in IL-31-induced scratching (Fig. 5D). One possible explanation is that Tmem184b expression at high levels may be promoting apoptosis. In support of this model, we see decreased expression of apoptotic pathway components when Tmem184b is absent and restoration of these components upon Tmem184b re-expression in cultured DRGs (data not shown). Another possibility is that Tmem184b over-expression may promote degeneration of pruriceptive axons. Future

experiments deleting *Tmem184b* solely in adults would be necessary to clarify roles for Tmem184b in long-term maintenance of pruriceptors.

In summary, we show that Tmem184b activity critically affects the development of pruriceptive neurons in mouse DRG and that this effect is likely due to its ability to induce components of Wnt signaling during neurogenesis. Our data illuminates a new key regulatory step in the processes controlling the establishment of diversity in the somatosensory system.

## Materials and Methods

### Animal Models

All animal treatment was approved by the Institutional Animal Care and Use Committee at the University of Arizona (protocol # 17-216). Tmem184b gene-trap mice have been described previously.(Bhattacharya et al., 2016) Mice were bred to *Sst*$^{Cre}$ and Rosa-Flox-stop-Flox-tdTomato (also called Ai9) (lines 013044 and 007909, Jackson Laboratory, Bar Harbor, ME) for histological quantification of the C2 population. Only heterozygous *Sst*$^{Cre}$ mice were used for experiments due to the possible disruption of normal somatostatin expression in homozygous Cre mice.

### RNA sequencing

Total RNA was isolated from adult DRG from 6-month old mutant and wild-type mice (4 per genotype, mixed male and female groups) using the RNaqueous Micro kit (Ambion). All DRGs were pooled for each sample to obtain enough RNA for analysis. Following total RNA extraction, samples were ethanol precipitated to increase purity. Library preparation and sequencing was performed at the Washington University Genome Technology Access Center (GTAC). Data were analyzed using Salmon and DeSeq2 (on our servers or with Galaxy, www.usegalaxy.org). Volcano plots were generated in RStudio; heatmaps of genes for which adjusted P values were less than 0.05 were created using R or with Cluster 3.0 and Java

Treeview. To create heatmaps of normalized counts, hierarchical clustering was used in Cluster3.0 to arrange genes by expression similarity. For embryonic DRG analysis, total RNA was isolated using TRIzol and library preparation and sequencing was performed by Novogene; identical analysis methods were used. For bioinformatics analysis, we used Panther's over-representation analysis of biological processes (complete) (http://www.pantherdb.org/) as well as Enrichr (www.enrichr.com). Fold enrichment was calculated as the number of statistically significantly expressed genes from the input dataset divided by the number of genes expected from the entire mouse reference genome. Expected genes in a GO category calculated by applying the proportion of all genes in reference genome associated with a GO category to the number of genes in input dataset. Significance calculated by Fisher's exact test with a BHM FDR ≤ 0.05. For timecourse and *in vitro* rescue RNAseq analysis, PCA analysis revealed occasional samples that did not cluster with their cohort; these were excluded from downstream DeSeq2 analysis while maintaining independent biological replicates of ≥ 3 for all experiments.

**Cytokine Injections and Behavior Analysis**

Mice were at least 8 weeks old at the time of injection. For itch experiments, both males and females of approximately equal quantities were used and data were pooled. Littermate controls were used, and videos were captured early in the morning to minimize mice falling asleep during videotaping. Mice were acclimated to behavioral chambers (red Rat Retreats, Bioserv) for one hour, removed from the chamber briefly for injections of either IL-31 (Peprotech, 3 nmol in 10 microliters of PBS for cheek injections or 300 μM for nape injections, depending on experiment), chloroquine (concentration), or 0.9% saline alone, and returned to the chamber, at which time videotaping began. Analysis was done blinded to genotype and injected substance. Scratching bouts were tallied for 30 minutes post-injection. If a mouse did not move for 10% or more of the video (≥ 3 min), it was excluded from analysis. Tail flick, hot plate, and Von Frey testing methods have been previously described. (Bannon and Malmberg, 2007; Chaplan et al.,

1994; Hargreaves et al., 1988) For pain and mechanical threshold testing, the experimenter was blinded to genotype, and males and females were separated during analysis.

**AAV Injection**

Custom AAV9 was built and titered by Vector Biolabs. Viruses were intrathecally injected (10ul, 2.0 x 10^6 virus particles/mL) at 8 to 9 weeks of age. Each mouse received intradermal (i.d.) saline injections 3 weeks after AAV delivery, and one week later received i.d. IL-31 injections. One Tmem184b mutant mouse with ~10x average scratching behavior to both saline and IL-31 was treated as an outlier and removed from our analysis.

**DRG Immunohistochemistry and Image Analysis**

Isolated ganglia or spinal cords were fixed with 4% paraformaldehyde for 1 hour, immersed in 30% sucrose overnight (4°C), and embedded in OCT cryo-compound (Tissue-Tek® O.C.T.) using isopentane cooled with dry ice. Spinal cords were dissected into segments containing two spinal segments (e.g. cervical 1 and 2). DRG cryosections (14 µm thickness) or spinal cord sections (20 µm thickness) were-mounted onto charged microscope slides. Following washes in PBST and 1 hour of blocking in 5% goat serum in PBST, sections were incubated overnight at 4°C with rabbit NeuN (1:250, Proteintech), or for 1 hour with Alexa Fluor® 488 Mouse anti-β-Tubulin, Class III (BD Pharmingen). Secondary antibody for NeuN was goat anti-rabbit Alexa Fluor 633 (Thermo Fisher). Sections were mounted in Vectashield (Vector Biolabs). Spinal cords were imaged with a ZEISS AxioZoom V16 Fluorescent Microscope. DRGs were imaged using a ZEISS Axio Observer Z1 or LSM880 inverted confocal microscope. For DRG counting, only neurons with a visible NeuN-positive nucleus in the section were counted. For each genotype, n = 5 mice. For each mouse, ≥800 neurons were counted.

**Neuronal Culture**

For adult neurons, ganglia from all spinal levels were pooled in DMEM on ice, followed by digestion with Liberase TM (Roche) and 0.05% Trypsin (Gibco). Neurons were dissociated with a P1000 pipette tip, spotted in dense culture spots (20uL) on poly-D-lysine (Sigma) and laminin

coated chambered coverglass (Nunc) or 100mm glass coverslips, and grown overnight in Dulbecco's Modified Eagle Medium (Gibco) with 10% fetal bovine serum (Atlas Biologicals) and Penicillin/Streptomycin (Gibco). For embryonic DRG culture, ganglia were dissociated with Trypsin, triturated with a P1000 pipette tip, and plated in 5-10 μl spots in a 24-well dish previously coated with poly-D-lysine and laminin. Media contained B27 (Gibco), 5-fluoro-deoxy-uridine (FDU) and nerve growth factor (NGF) (Invitrogen). Half of the media volume was exchanged every 5 days until cells were collected for analysis.

**Calcium Imaging**

Adult DRG neurons were imaged either with Fluo-4 dye on a Zeiss Observer Z1 microscope, or with Fura-2 dye on an Olympus BXW microscope under a 10X immersion objective lens with a filter wheel and Hamamatsu camera, each with a frame rate of one image/3 sec. Data shown used ratiometric, perfusion based Fura-2 imaging with the exception of IL-31 and chloroquine, which used Fluo-4 due to quantity constraints (IL-31) or autofluorescence in UV wavelengths (chloroquine). Fluorescence videos were acquired via Zeiss or HCImage Software, processed and analyzed using MATLAB, and RStudio for quantification of fluorescent responses. We used a custom-written R script to identify neurons via responses to high potassium in each experiment. Responses to individual agonists were determined manually for all neurons. Each agonist was evaluated using cultures from at least 3 mice, and most agonist-genotype combinations have >1000 neurons analyzed (minimum 659, maximum 2333). Coverslips with extensive motion or other artifacts were excluded from analysis. Perfusion artifacts (single frame spikes) were identified and removed prior to analysis.

**Statistics**

All statistical analysis was performed in Graphpad Prism. Where applicable for multiple test corrections, all False-Discovery Rates determined with Benjamini-Hochberg Method (BHM); thresholds set at (FDR) ≤ 0.05. For all figures, asterisks indicate $p < 0.05$ (*), $p < 0.01$ (**), p <

0.001 (***), or $p < 0.0001$ (****). For calcium imaging, binomial response counts were analyzed using two-sided Chi-square tests. In all experiments, independent samples were measured.

**Data availability**

The data sets generated and analyzed in the current study will be deposited at NCBI GEO upon publication and linked to this manuscript.

**Code availability**

All custom-written code in R and MATLAB for calcium imaging and RNAseq analysis will be made available on GitHub upon publication (https://github.com/martharcb/Fluo4_R.git and https://github.com/eriklarsen4/ggplot-scripts).

**Acknowledgements**

We would like to thank Dr. Aubin Moutal for assistance with adult DRG cultures and calcium imaging. This work was supported by the University of Arizona (Technology and Research Incentive Fund) and R01 NS105680 to M.R.C.B.

**Author Contributions**

E.L. and M.B. designed the experiments. E.L. and M.B. performed RNAseq analysis and calcium imaging and analysis. T.C., J.F., E.L., C.M. and M.B. performed behavioral experiments. E.L., M.M., T.C, B.M., N.K., E.W., C.J., H.G. and M.B. analyzed behavior videos. T.L. performed intrathecal AAV injections. H.H. and R.K. supported experiments in their laboratories and offered guidance on the project. E.G.L. and M.R.C.B. wrote the manuscript.

**Declaration of Interests**

The authors declare no competing interests.

**References**

Acton, D., Ren, X., Di Costanzo, S., Dalet, A., Bourane, S., Bertocchi, I., Eva, C., and Goulding, M. (2019). Spinal Neuropeptide Y1 Receptor-Expressing Neurons Form an Essential Excitatory Pathway for Mechanical Itch. Cell Rep. *28*, 625-639.e6.

Bannon, A.W., and Malmberg, A.B. (2007). Models of Nociception: Hot-Plate, Tail-Flick, and Formalin Tests in Rodents. In Current Protocols in Neuroscience, (John Wiley & Sons, Inc.), p.

Bhattacharya, M.R.C., Geisler, S., Pittman, S.K., Doan, R.A., Weihl, C.C., Milbrandt, J., and DiAntonio, A. (2016). TMEM184b promotes axon degeneration and neuromuscular junction maintenance. J. Neurosci. *36*.

Bourane, S., Duan, B., Koch, S.C., Dalet, A., Britz, O., Garcia-Campmany, L., Kim, E., Cheng, L., Ghosh, A., Ma, Q., et al. (2015). Gate control of mechanical itch by a subpopulation of spinal cord interneurons. Science *350*, 550–554.

Cevikbas, F., Wang, X., Akiyama, T., Kempkes, C., Savinko, T., Antal, A., Kukova, G., Buhl, T., Ikoma, A., Buddenkotte, J., et al. (2014). A sensory neuron-expressed IL-31 receptor mediates T helper cell-dependent itch: Involvement of TRPV1 and TRPA1. J. Allergy Clin. Immunol. *133*, 448–460.

Chaplan, S.R., Bach, F.W., Pogrel, J.W., Chung, J.M., and Yaksh, T.L. (1994). Quantitative assessment of tactile allodynia in the rat paw. J. Neurosci. Methods *53*, 55–63.

Chiu, I.M., Barrett, L.B., Williams, E.K., Strochlic, D.E., Lee, S., Weyer, A.D., Lou, S., Bryman, G.S., Roberson, D.P., Ghasemlou, N., et al. (2014). Transcriptional profiling at whole population and single cell levels reveals somatosensory neuron molecular diversity. Elife *3*.

Dillon, S.R., Sprecher, C., Hammond, A., Bilsborough, J., Rosenfeld-Franklin, M., Presnell, S.R., Haugen, H.S., Maurer, M., Harder, B., Johnston, J., et al. (2004). Interleukin 31, a cytokine produced by activated T cells, induces dermatitis in mice. Nat. Immunol. *5*, 752–760.

Dong, X., and Dong, X. (2018). Peripheral and Central Mechanisms of Itch. Neuron *98*, 482–494.

Garcia-Morales, C., Liu, C.-H., Abu-Elmagd, M., Hajihosseini, M.K., and Wheeler, G.N. (2009). Frizzled-10 promotes sensory neuron development in Xenopus embryos. Dev. Biol. *335*, 143–155.

Hargreaves, K., Dubner, R., Brown, F., Flores, C., and Joris, J. (1988). A new and sensitive method for measuring thermal nociception in cutaneous hyperalgesia. Pain *32*, 77–88.

Huang, C., Lu, F., Li, P., Cao, C., and Liu, Z. (2017). Tlx3 Function in the Dorsal Root Ganglion is Pivotal to Itch and Pain Sensations. Front. Mol. Neurosci. *10*, 205.

Huang, J., Polgár, E., Solinski, H.J., Mishra, S.K., Tseng, P.-Y., Iwagaki, N., Boyle, K.A., Dickie, A.C., Kriegbaum, M.C., Wildner, H., et al. (2018). Circuit dissection of the role of somatostatin in itch and pain. Nat. Neurosci. *21*, 707–716.

Kondo, T., Matsuoka, A.J., Shimomura, A., Koehler, K.R., Chan, R.J., Miller, J.M., Srour, E.F., and Hashino, E. (2011). Wnt signaling promotes neuronal differentiation from mesenchymal stem cells through activation of Tlx3. Stem Cells *29*, 836–846.

Lallemend, F., and Ernfors, P. (2012). Molecular interactions underlying the specification of sensory neurons. Trends Neurosci. *35*, 373–381.

Lee, H.Y., Kléber, M., Hari, L., Brault, V., Suter, U., Taketo, M.M., Kemler, R., and Sommer, L. (2004). Instructive Role of Wnt/β-Catenin in Sensory Fate Specification in Neural Crest Stem Cells. Science (80-. ). *303*, 1020–1023.

Li, C.-L., Li, K.-C., Wu, D., Chen, Y., Luo, H., Zhao, J.-R., Wang, S.-S., Sun, M.-M., Lu, Y.-J., Zhong, Y.-Q., et al. (2016a). Somatosensory neuron types identified by high-coverage single-cell RNA-sequencing and functional heterogeneity. Cell Res. *26*, 83–102.

Li, C.-L., Li, K.-C., Wu, D., Chen, Y., Luo, H., Zhao, J.-R., Wang, S.-S., Sun, M.-M., Lu, Y.-J., Zhong, Y.-Q., et al. (2016b). Somatosensory neuron types identified by high-coverage single-cell RNA-sequencing and functional heterogeneity. Cell Res. *26*, 83–102.

Liu, Q., Tang, Z., Surdenikova, L., Kim, S., Patel, K.N., Kim, A., Ru, F., Guan, Y., Weng, H.-J., Geng, Y., et al. (2009). Sensory neuron-specific GPCR Mrgprs are itch receptors mediating

chloroquine-induced pruritus. Cell *139*, 1353–1365.

Lopes, C., Liu, Z., Xu, Y., and Ma, Q. (2012). Tlx3 and Runx1 act in combination to coordinate the development of a cohort of nociceptors, thermoceptors, and pruriceptors. J. Neurosci. *32*, 9706–9715.

Oetjen, L.K., Mack, M.R., Feng, J., Whelan, T.M., Niu, H., Guo, C.J., Chen, S., Trier, A.M., Xu, A.Z., Tripathi, S. V, et al. (2017). Sensory Neurons Co-opt Classical Immune Signaling Pathways to Mediate Chronic Itch. Cell *171*, 217-228.e13.

Pagani, M., Albisetti, G.W., Sivakumar, N., Wildner, H., Santello, M., Johannssen, H.C., and Zeilhofer, H.U. (2019). How Gastrin-Releasing Peptide Opens the Spinal Gate for Itch. Neuron *103*, 102-117.e5.

Pan, H., Fatima, M., Li, A., Lee, H., Cai, W., Horwitz, L., Hor, C.C., Zaher, N., Cin, M., Slade, H., et al. (2019). Identification of a Spinal Circuit for Mechanical and Persistent Spontaneous Itch. Neuron *103*, 1135-1149.e6.

Raisa Eng, S., Gratwick, K., Rhee, J.M., Fedtsova, N., Gan, L., and Turner, E.E. (2001). Defects in sensory axon growth precede neuronal death in Brn3a-deficient mice. J. Neurosci. *21*, 541–549.

Sharma, N., Flaherty, K., Lezgiyeva, K., Wagner, D.E., Klein, A.M., and Ginty, D.D. (2020). The emergence of transcriptional identity in somatosensory neurons. Nature *577*, 392–398.

Shen, C., Li, L., Zhao, K., Bai, L., Wang, A., Shu, X., Xiao, Y., Zhang, J., Zhang, K., Hui, T., et al. (2018). Motoneuron Wnts regulate neuromuscular junction development. Elife *7*.

Solinski, H.J., Kriegbaum, M.C., Tseng, P.-Y., Earnest, T.W., Gu, X., Barik, A., Chesler, A.T., and Hoon, M.A. (2019). Nppb Neurons Are Sensors of Mast Cell-Induced Itch. Cell Rep. *26*, 3561-3573.e4.

Usoskin, D., Furlan, A., Islam, S., Abdo, H., Lönnerberg, P., Lou, D., Hjerling-Leffler, J., Haeggström, J., Kharchenko, O., Kharchenko, P. V, et al. (2015). Unbiased classification of sensory neuron types by large-scale single-cell RNA sequencing. Nat. Neurosci. *18*, 145–153.

Wilson, S.R., Thé, L., Batia, L.M., Beattie, K., Katibah, G.E., McClain, S.P., Pellegrino, M., Estandian, D.M., and Bautista, D.M. (2013). The epithelial cell-derived atopic dermatitis cytokine TSLP activates neurons to induce itch. Cell *155*, 285–295.

Yee, D.C., Shlykov, M.A., Västermark, A., Reddy, V.S., Arora, S., Sun, E.I., Saier, M.H., and Jr. (2013). The transporter-opsin-G protein-coupled receptor (TOG) superfamily. FEBS J. *280*, 5780–5800.

Zheng, Y., Liu, P., Bai, L., Trimmer, J.S., Bean, B.P., and Ginty, D.D. (2019). Deep Sequencing of Somatosensory Neurons Reveals Molecular Determinants of Intrinsic Physiological Properties. Neuron *103*, 598-616.e7.

## Figure Legends

**Figure 1. Tmem184b is Required for Expression of Pruriceptor-Specific Markers.** (A) Volcano plot of RNA sequencing data. Gold, differentially expressed (DEGs) (n = 381 genes); navy shows a subset of itch-related DEGs (n = 24 genes); gray, non-differentially expressed genes (n = 12,550 genes). Benjamini-Hochberg Method-derived FDR; FDR ≤ 0.05. (B) Heatmap showing aligned, variance-normalized samples (N = 4 per genotype), and DEGs of interest independently clustered by expression similarity. (C) Venn diagram of selected sensory neuron expressed DEGs showing their specific expression in subsets of nociceptors. (D) Over-represented Panther pathways (FDR ≤ 0.05) in downregulated DEGs.

**Figure 2**. **Altered neuronal responses cause behavioral loss of IL-31 mediated itch.** (A-E) Behavioral analysis of itch and pain in Tmem184b mutant mice. (A) IL-31 induced scratching responses (p = 0.014). (B) Chloroquine-induced scratching responses (p = 0.073). (C) Hot plate analysis (female, p = 0.3404; male, p = 0.694). (D) Tail flick analysis (Female: p = 0.762; Male: p = 0.769). (E) Baseline mechanical thresholds (Female: p = 0.735; Male: p = 0.983). All data presented as mean ± SD. For (A-B), n= 7-12 for itch agonists and 5-6 for saline controls, and significance evaluated with one-way ANOVA. For nociceptive and mechanical evaluation (C-E), n= 8-14 animals per genotype and sex, and significance evaluated using two-tailed, unpaired t-test. (F-L) Calcium imaging population analysis for different nociceptor and pruriceptor specific agonists. Percent responders are shown for (F) Capsaicin (1μM), a TRPV1 agonist, (G) AITC (200μM), a TRPA1 agonist, (H) β-alanine (5mM), an MRGPRD agonist, (I) CYM5442 (250μM), an S1PR1 agonist, (J) LY344862 (2.5μM), an HTR1F agonist, (K) IL-31 (1μM), and IL31RA/Osmr agonist, and (L) chloroquine (CQ, 200μM), an MRGPRA3 agonist. Statistical significance was calculated using two-tailed Chi-square analysis. Inset numbers are total

analyzed neurons for each agonist and come from at least three mice per genotype. (M) Average IL-31 response calculated from wild type (blue) and mutant (orange) neurons classified as IL-31 responders. Wild type (n = 19) and mutant (n = 24) neurons cultured and imaged on the same day with the same solutions were averaged.

**Figure 3. Tmem184b regulates key developmental pathways in somatosensory neurons.** A, Genetic labeling of Sst-Cre somatosensory neurons (magenta) expressing tdTomato in Tmem184b gene trap mice. Green indicates NeuN (neurons). B, Percent of neurons labeled with Sst-Cre>Ai9 in wild type and Tmem184b-mutant mice. n=5-6 mice and ≥800 neurons analyzed per mouse. Data presented as mean ± SD (7.20 ± 2.00, 4.21, ± 1.74, t = 2.52, p = 0.036, unpaired t test) C, Quantification of embryonic day 13 (E13) DRG Tmem184b transcripts per million (TPM) reads. Error bar shows SEM; significance calculated by student's t-test, p = 0.0061. N = 3 embryos per genotype analyzed. D, MA plot of RNAseq E13 Tmem184b GT/GT dorsal root ganglia, showing fold change versus average transcript expression across all replicates. Colors: gold, differentially expressed genes (DEGs); blue, neuron differentiation DEGs as annotated in gene ontology (Panther); gray, non-DEGs. E, Enriched GO Biological Processes in E13 differentially expressed genes (gold from D). Top 10 most significantly enriched pathways (by adjusted P-value) are shown. *, FDR < 0.05. F, Heatmap of selected, differentially expressed neuron differentiation genes at E13. (G-K) Normalized counts of individual genes from RNAseq analysis of E13, P0, and P10 mutant and wild type mouse dorsal root ganglia. n = 3-4 mice per time-point and genotype. Asterisks indicate statistical significance as calculated by DESeq2 (Wald Test with FDR ≤ 0.05). Data presented as mean ± SEM. (G) *Wnt3a* (q < 0.0001). (H) *Neurog1* (q < 0.0001). (I) *Neurog2* (q < 0.0001). (J) *Sst* (q = 0.0082 for P0, q <0.0001 for P10). (K) *Il31ra* (q =0.09).

**Figure 4. Tmem184b controls expression of Wnt signaling components in embryonic DRG neurons.** (A) Schematic of the experimental design. Samples from dissociated DRG neurons at DIV 0 (N = 4 per group) and DIV 14 (N = 5 per group) were collected for RNAseq analysis. (B-C), Volcano plots showing (B) DIV14 Tmem184b-mutant vs DIV14 WT and (C) DIV14 rescue vs DIV14 mutant transcript expression. Gray dots show genes not significantly altered. Navy, downregulated genes (Adj P ≤ 0.01); gold, upregulated genes (Adj P ≤ 0.01). (D) Genes both downregulated in DIV14 mutant eDRGs (B, navy) and upregulated in rescued DIV14 mutant eDRGs (C, gold) were analyzed using Panther gene ontology over-representation analysis. Fold enrichment when compared to all mouse transcripts is shown for all processes with enrichment scores >5. *, FDR < 0.05 and **, FDR <0.01. (E) Expression of genes annotated as Wnt signaling effectors, normalized to WT DIV14 levels. Green genes positive regulate Wnt signaling (15 genes), while red genes negatively regulate Wnt signaling (4 genes).

**Figure 5. *In vivo* re-expression of Tmem184b in adult mutant ganglia does not increase IL-31 responses.** (A) Schematic of the adult rescue experiment. (B) DRG from cervical regions of AAV-injected mice, showing successful virus infection and spread between C1-C10 (mCherry). (C) Spinal cord expression of mCherry in both incoming DRG processes (left) and in grey matter (right). (D) Wild type and Tmem184b mutant scratch responses, sorted by AAV type and agonist (IL-31, filled squares; saline, open circles). Analysis by two-way ANOVA with Tukey's correction for multiple comparisons. P values in wild type: mCherry saline vs IL-31, p = 0.0005; IL-31 mCherry vs *Tmem184b* virus, p = 0.0024. P values in mutant: mCherry saline vs IL-31, p = 0.101; IL-31 mCherry vs Tmem184b virus, p = 0.5.

**Supplemental Figure 1. Genes with known roles in development or maturation of sensory neurons are differentially affected by Tmem184b loss.** For all graphs, * indicates $p<0.05$, ** indicates $p<0.01$, *** indicates $p<0.01$, and **** indicates $p<0.0001$. (A) Wnt associated genes Tlx3, Gsk3β, and β-Catenin. (B) Runx transcription factors Runx1, Runx2, and Runx3. (C) Neuronal subtype specific genes MrgprA3 (chloroquine receptor), Cysltr2 (β-alanine receptor), Htr1f (serotonin receptor subtype 1f), and Nppb (natriuretic polypeptide B, also called BNP). (D) Neurotrophin receptors TrkA, TrkB, and TrkC. (E) JNK kinases JNK1, JNK2, and JNK3.

# Fig 1. Tmem184b is Required for Expression of Pruriceptor-Specific Markers

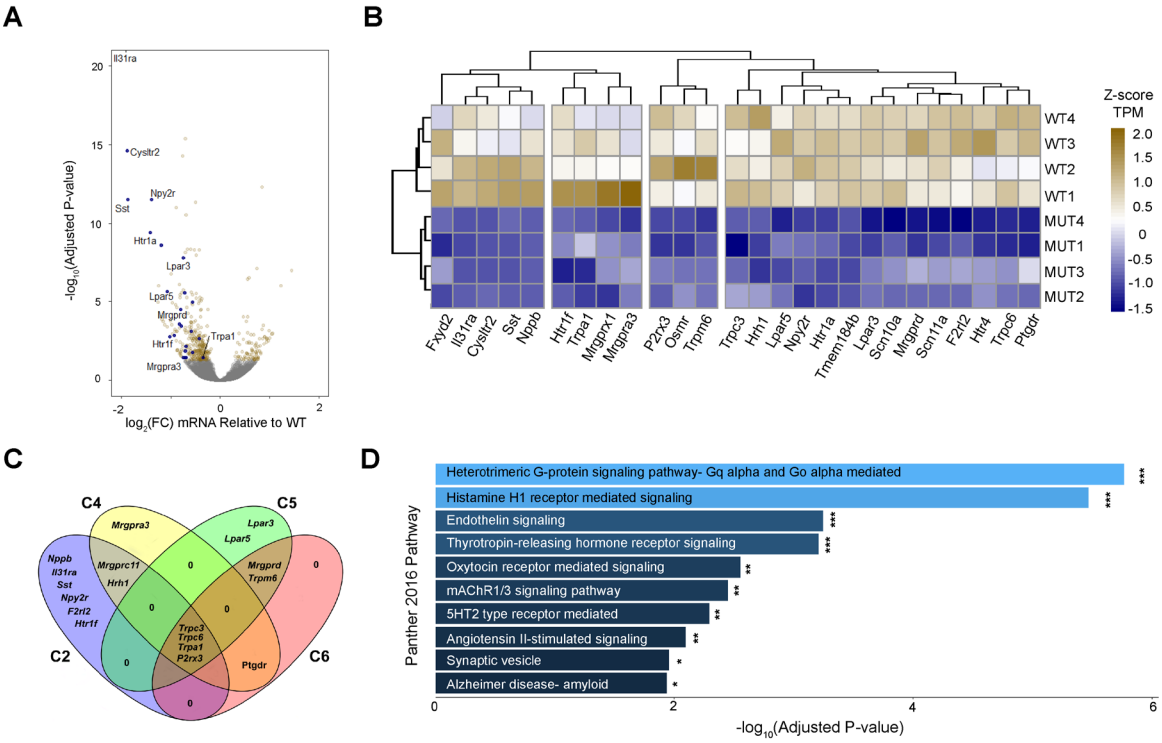

## Figure 2. Altered Neuronal Responses Cause Behavioral Loss of IL-31-Mediated Itch

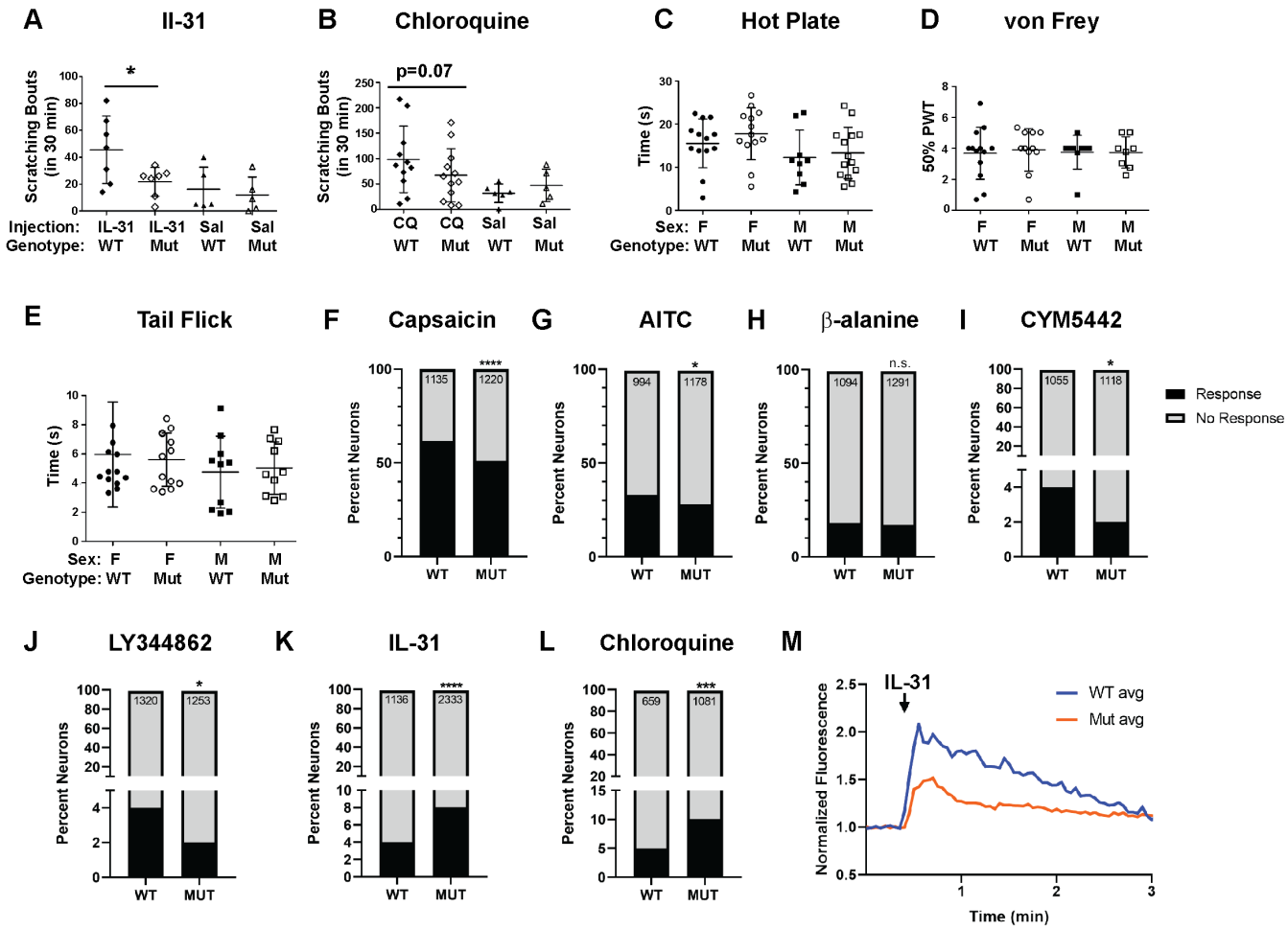

**Figure 3. Tmem184b regulates key developmental pathways in somatosensory neurons**

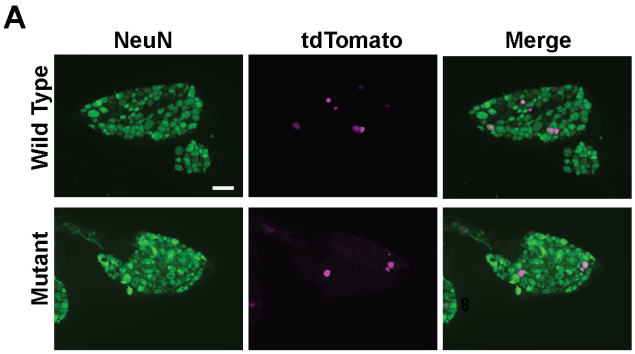


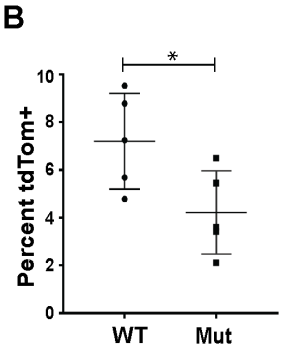


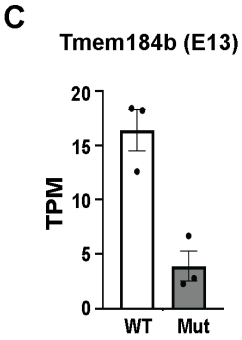


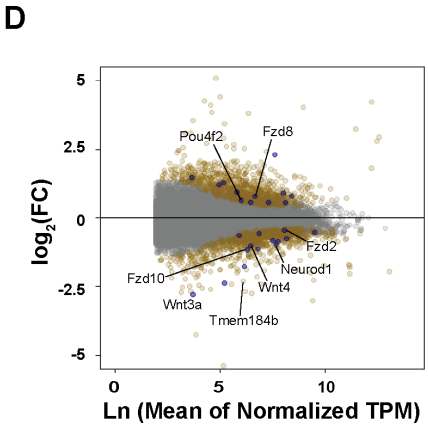


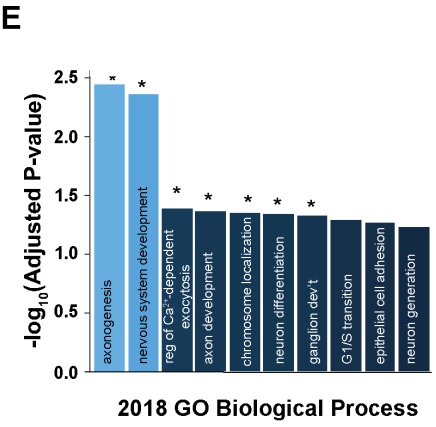


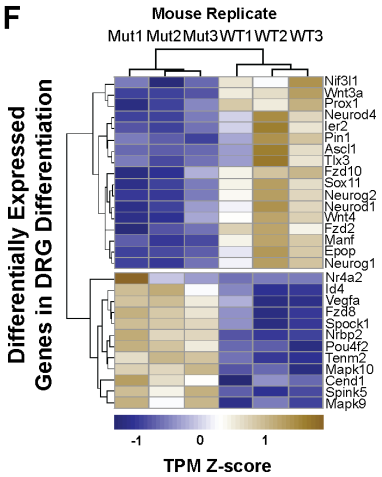


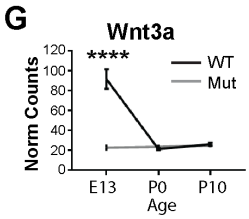


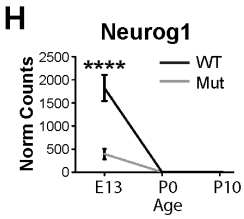


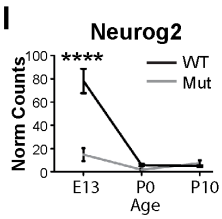


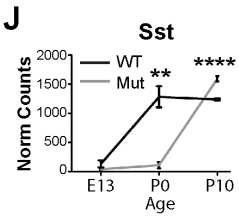


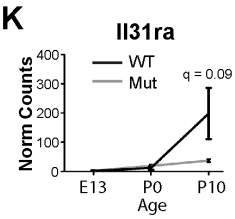

# Fig 4. Tmem184b controls expression of Wnt signaling components in embryonic DRG neurons

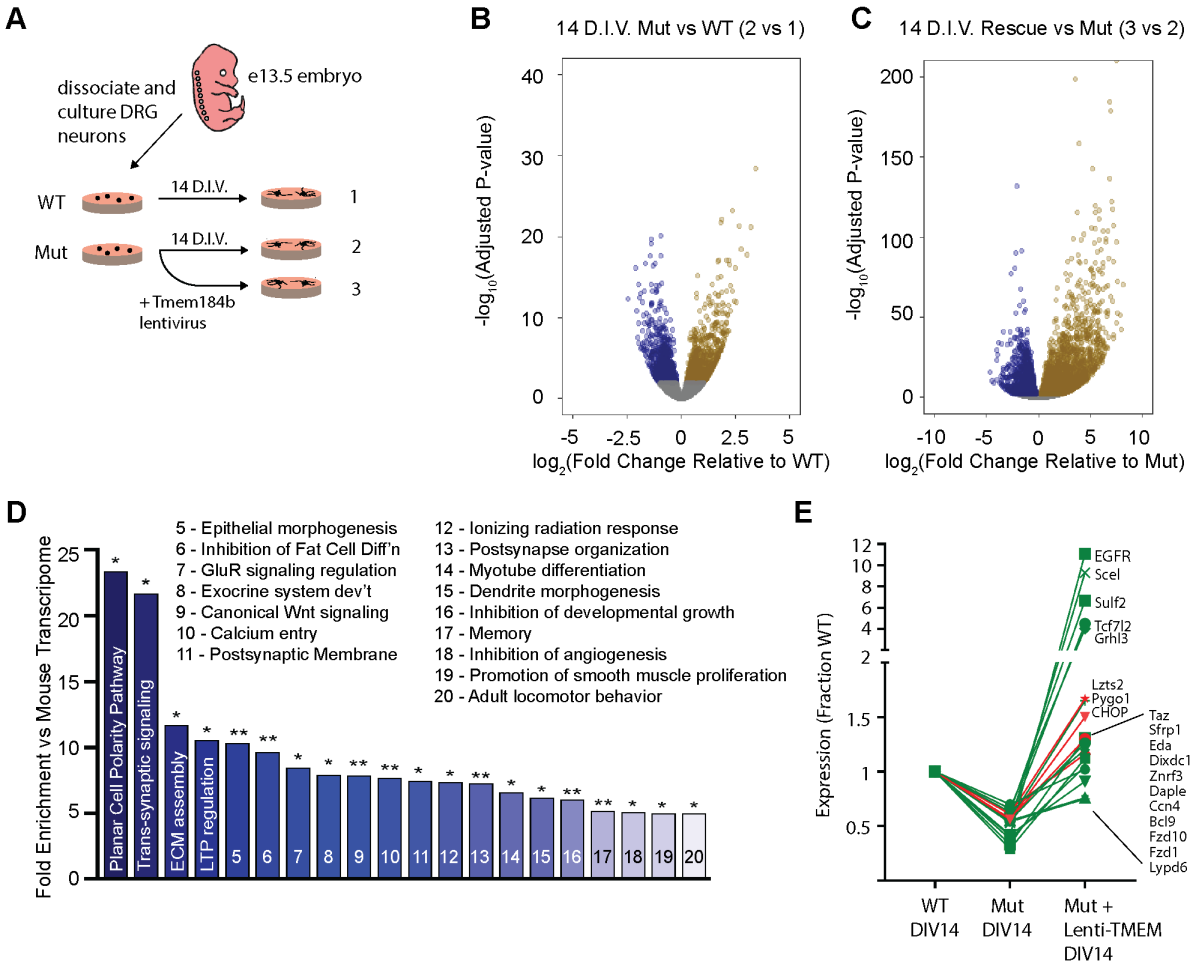

Figure 5. In vivo re-expression of Tmem184b in adult mutant ganglia does not increase IL-31 responses.

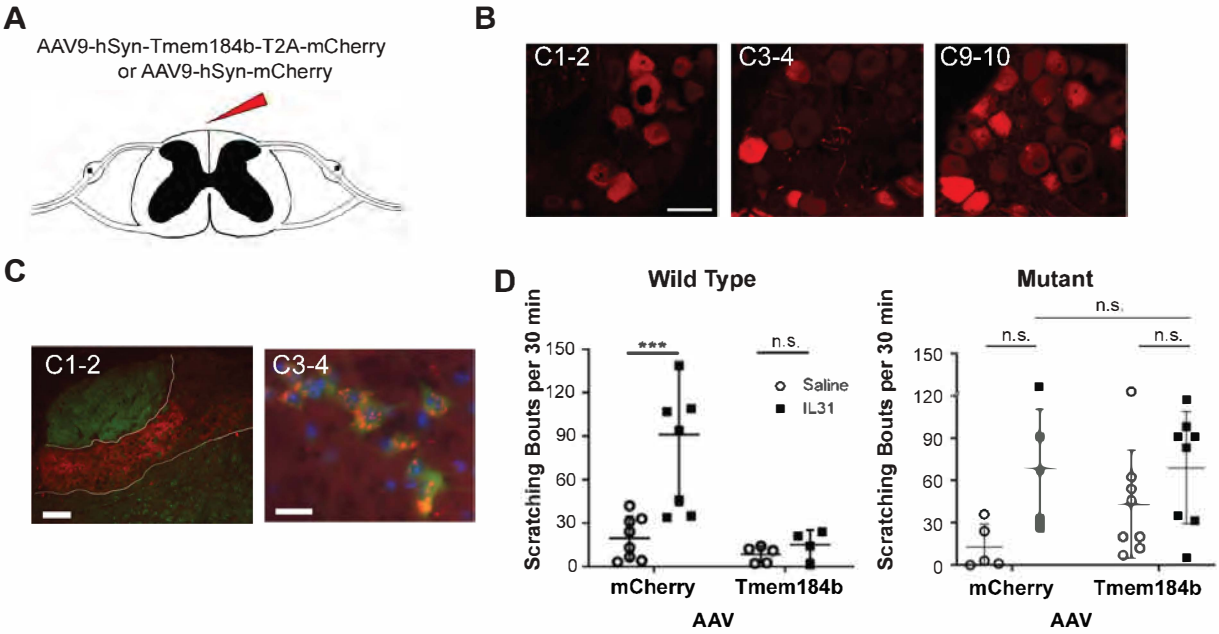
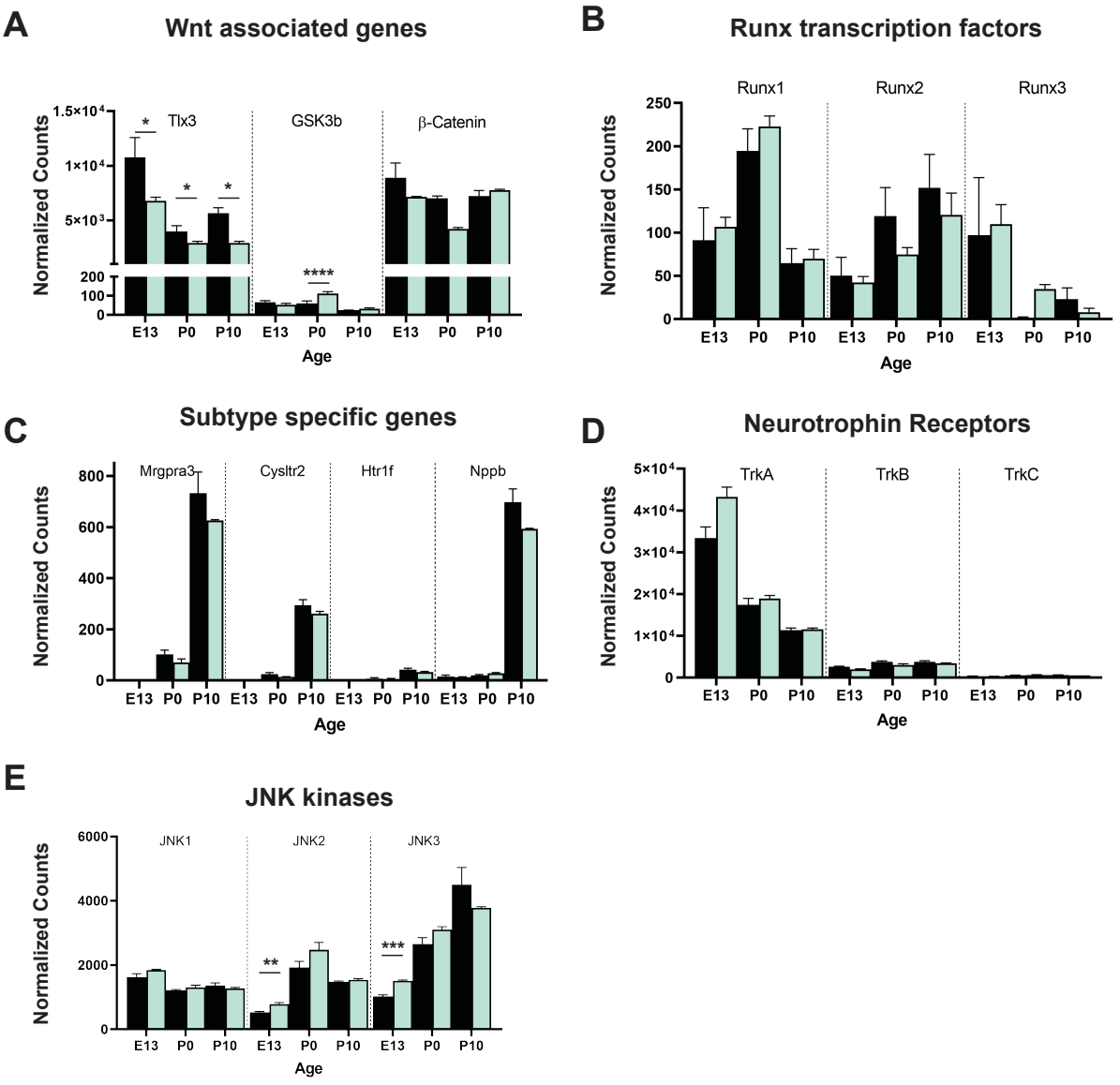
**Supplemental Figure 1. Genes with known roles in development or maturation of sensory neurons are differentially affected by Tmem184b loss.**